

Utilizing Project Management Techniques for Project Selection in the Design of Snowmobile Modifications to reduce Emissions and Noise

Frank Siracusa, Ryan Fix, Nick McCormick, Ryan Derrick, Austin Iverson, and Brent Williams

Abstract

For the 2018 Clean Snowmobile Challenge, the University of Minnesota Twin Cities team has focused on the further development of past designs along with the transfer to a new base snowmobile. An emphasis was placed on project management techniques and team organization to ensure the timely completion of projects that had caused schedule variances in the past. In order to meet the goals of the challenge of improving emissions, noise, and fuel economy, the team has chosen to make use of a catalytic converter with a custom muffler, a simplified engine management strategy, and further work on the impedance tube for testing acoustical properties.

Innovations

The University of Minnesota Clean Snowmobile Team has decided to begin a new design cycle using a different base snowmobile this year. Due to many factors, but with a high importance on performance and enthusiast appeal, the team has selected a 2016 Polaris Switchback Adventure as a basis for design. This choice retains a very similar 600cc 2-stroke engine to the entries of previous years.

Another departure in the design was moving away from a standalone ECU to tuning using a Power Commander V piggyback unit from Dynojet Research. This change drastically impacted the project management of the team, and was representative of the year's project selection process, which is detailed in the Team Organization and Time Management Section.

A new muffler was designed to fit both a differently sized catalyst and the smaller amount of room available underneath the side panels of the new sled. The catalyst used on the 2018 entry was enlarged compared to the 2017 design to help improve conversion of emissions.

Previous work on an impedance tube was furthered this year by adding a second microphone to take reflections off of the sound deadening material into account, and better quantify the effects of adding coatings and foams to the sled.

Team Organization and Time Management

The team was first formed in the summer of 2014, and first attended the Clean Snowmobile Challenge in spring 2015. As a newer team to the competition, the team's project management strategy has changed a lot over the last four years, with many approaches attempted being unsuccessful. This year, the team realized that changes to the team

structure and project management were necessary to help facilitate the completion of projects on time.

The first change made was in team organization. The team officer roles were changed and redefined to help spread workload and give team leadership better visibility of how projects are coming along.

Name	Position	Responsibilities
Frank Siracusa	President	Manage team, sponsorship, outreach events, grants
Andrew Michel	Vice President	Plan budget, POs, MSRP
Ryan Fix	Project Manager	Manage team leads, create schedule
Frank Siracusa	Engine Team Lead	Manage engine, exhaust, and tuning projects
Max Mraz	Electrical Team Lead	Manage wiring, sensors, dyno
Brent Williams	Chassis Team Lead	Manage chassis, passing tech, suspension

Figure 1: 2018 team leadership roles and responsibilities.

This team organization creates a chain of accountability through the project and team leads associated with each project, making it much easier for the project manager to ascertain how well things are going relative to the original schedule. It also creates specific positions for taking care of team finances and other administrative tasks, leaving more time open for other members to work on their designs without distraction.

Along with managing team finances, the president and vice president help plan the many outreach events the team participates in each year. For on-campus outreach to other students, the team attends freshmen welcome week, a student organization fair every semester, and participates in student board meetings. The team also attends some meetings put on by the Twin Cities region SAE, the Minnesota State Fair, and Sno Barons Hay Days for industry and community outreach.

Project Selection

The team has always kept schedules in the form of calendars, Gantt charts, and other organizational tools, but has still had difficulty in meeting set deadlines. Multiple changes in the direction or scope of projects would make the schedules obsolete and hard to keep track of. Because of this, the team put a focus on finding new project management techniques that were more applicable to their situation.

The tools chosen for use by the team center around project selection and risk management. A large problem identified in previous years was the selection of projects that took a large amount of time, and did not have a large payoff. At the beginning of this design cycle, the team decided to create an impact effort matrix to help score and select potential projects.

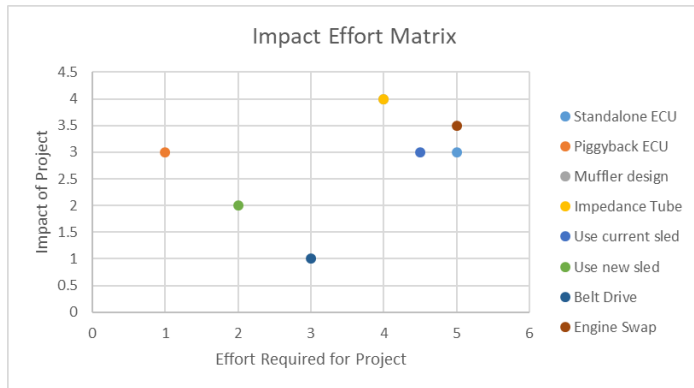


Figure 2: An example of an Impact Effort Matrix made by the team early in the design cycle to help select projects. Effort and impact are ranked.

This matrix was used very early in the design cycle, and the results found made a large impact. After thinking about the real benefit given by the completion of some projects, it was clear that some past projects should be abandoned in favor of projects with more potential to help the team. One such decision was to start with a new base snowmobile. If the team had selected to use the 2017 entry again, there would be a significant amount of wiring work and tuning necessary to reach a stock level of performance. Starting with a new sled and implementing a piggyback ECU would give the team much of the same benefit without anywhere near as much work. The belt drive conversion project, which had been around for a few years, but was never completed, was also abandoned because the amount of work necessary was too high to justify the time commitment. Even though some projects require high effort, like the impedance tube and muffler design, both rated at 4/5 effort and 4/5 impact, the high impact of the projects justified the time that would be spent completing them.

Another strategy the team utilized to ensure the completion of projects was risk identification and management. Although the team has had a dynamometer for the last few years, the team has yet to be able to obtain a space on campus to utilize it for tuning and collecting data. With the University of Minnesota-Twin Cities being in Minneapolis, the team also finds it difficult to find nearby areas to ride the sled for testing. Knowing this, along with the effort and payoff data, the team chose to move to a new snowmobile and a piggyback ECU to speed up the engine calibration process. Since the risk of not having the capability to spend much time calibrating was very likely to occur, the team chose to focus on other projects that would be able to gain more benefit, and mitigate the risk of the sled not running well at competition by having the ability to easily revert to the stock calibration.

Snowmobile Overview

Chassis	2016 Polaris Switchback Adventure
Engine	Polaris 600cc Cleanfire 2-Stroke
Fuel	Gasoline
Peak Horsepower	110 (estimated from specifications)
Track	Camsco Storm 150 137"
Muffler	3-chamber Student Designed
Skis	Stock
Sound Deadening	Flex Seal

Figure 3: Table of basic information about 2018 snowmobile.

The team chose a 2016 Polaris Switchback Adventure for the 2018 Clean Snowmobile Challenge. This selection was made in a large part based on the Polaris Axys chassis, that allowed the use of a 137" track instead of 121" for an increase in traction and handling with roughly the same weight as the previous year's entry.

The team chose to retain the 600cc 2-stroke engine due to the power to weight ratio provided as well as the identified risks and effort increased from an engine swap.

Catalyst Implementation

In an effort to substantially reduce the emissions of the snowmobile, a Heraeus three-way catalyst was implemented into the muffler redesign. The catalyst will convert hydrocarbons, CO, and NO_x into CO₂, H₂O, and N₂. It is important to develop the correct fuel to air ratio for proper use of a three-way catalyst. If the engine is running too lean, NO_x will not convert effectively. Conversely, running the engine too rich will result in incomplete conversion of hydrocarbons and CO. In general, the level of NO_x emissions from 2-stroke engines is low, especially compared to 4-strokes. The hydrocarbon emissions, however, tend to be very high. In Equation 1 from the Clean Snowmobile Challenge Rules, it can be seen that HC and NO_x carry a combined weight in emissions scoring [1].

$$E = \left[1 - \frac{(HC+NO_x)-15}{150} \right] * 100 + \left[1 - \left(\frac{CO}{400} \right) \right] * 100 \geq 100 \quad (EQ 1)$$

Where E is the E-Score, HC is hydrocarbons in g/Kw-hr, NO_x is nitrous oxides in g/Kw-hr, and CO is carbon monoxide in g/Kw-hr. Because HC and NO_x carry this combined weight, it was determined that the catalyst should focus on eliminating HC. It was for this reason that a Heraeus 1:20:1 catalyst was selected to be implemented into the exhaust system, which is the same as the Heraeus catalyst considered in 2017. As the catalyst last year was proven to not cause too much restriction in the exhaust, a 400 cells per square inch matrix was again used. This year, the team elected to increase the size of the catalyst from 70x75mm to 72x130mm. This increase in size increases

the surface area of catalyst that the exhaust contacts, and should increase conversion efficiency.

Emissions data was collected using the smaller size Heraeus catalyst at a few RPM levels using an E Instruments E8500 portable emissions analyzer.

	Idle	3000RPM	4000RPM
Temperature	698C	852C	856C
O2	5.4%	1.5%	0.8%
HC	0.02%	0.09%	0.06%
CO2	11%	15.4%	10.7%
CO	154ppm	754ppm	6852ppm
NO	65ppm	271ppm	21ppm

Figure 4: Emissions data taken post-catalyst using 70x75mm size.

HC	1.13%
CO2	2.0%
CO	3.05%
NO	40ppm
NO2	2ppm
NOx	43ppm

Figure 5: Emissions data taken at idle with no catalyst.

When the collected data is compared to data taken at idle with no catalyst, it is seen that total hydrocarbons in the exhaust are reduced from 1.13% to 0.02%, which is around 98.23% conversion efficiency.

Engine Management

For 2018, a Dynojet Power Commander V piggyback controller was used for engine calibration. This unit would make it possible to tune the engine while still having the option to revert to stock, which made it a low-risk, and, therefore attractive option for the team. It also required no wiring, which was a bonus for the team, who had found custom wiring harnesses to be a common failure point.

The ability to alter the calibration of the engine is important to emissions, fuel economy, and performance. As stated in the catalyst implementation section, the best conversion of emission and E-score will be obtained at a near stoichiometric air to fuel ratio. The Power Commander uses an O2 sensor and closed-loop control to ensure that the sled is running as close as possible to stoichiometric.

Ethanol Sensor and Conversion Circuit

In the past, the team has used standalone ECUs that were able to alter fuel and ignition curves based on a wide variety of inputs. This is the one area, for the 2018 team's purposes, that the Power Commander lacks in. As it will only accept an analog signal for an outside sensor, the ethanol sensor's digital signal was converted through a custom circuit so that the sensor could be implemented.

Exhaust Pressure Measurement

Sound is a pressure deviation from the ambient atmospheric pressure. The tone that a specific sound takes is determined by the frequency of its pressure wave, with low tones having low frequency and high tones having high frequencies. A snowmobile engine creates pressure waves through its exhaust system by opening and closing its exhaust ports. This is why the sound of an engine has a higher pitch at higher engine speeds. The University of Minnesota-Twin Cities Clean Snowmobile Team found and evaluated the frequency content of their engine/exhaust system to determine the frequencies a new muffler design should attenuate to reduce the volume of the engine noise. This was accomplished using pressure transducers located before and after the expansion pipe. A National Instruments data acquisition device accompanied by a LabVIEW program recorded the data which was analyzed using Microsoft Excel. During the test, the engine was not loaded and the operating speed was varied from 2000 to 8000 rotations per minute (RPM) in 500 RPM increments. A Fast Fourier Transform (FFT) was used to bring out the frequency content from the raw data.

Figure 6 shows the frequency content within the exhaust system at an engine operating speed of 7500 RPM. An increase in frequency content at 250 Hertz can be seen before the expansion pipe (pipe location). 250 Hertz is the frequency at which the exhaust ports open and close at an engine speed of 7500 RPM. However, a significant increase in frequency content just before the muffler (muffler location) is not seen until about 300 Hertz.

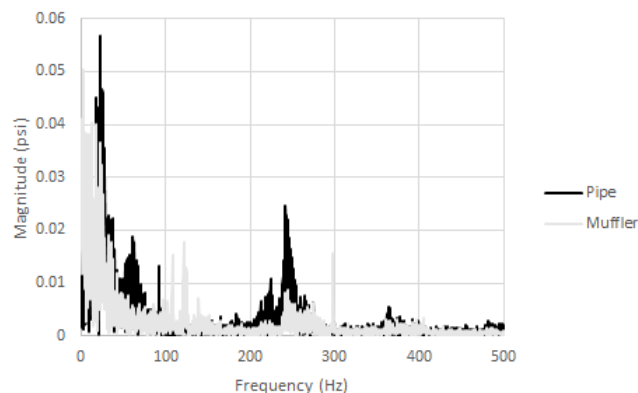


Figure 6: Frequency content of the exhaust system at an engine speed of 7500 RPM.

Figure 7 shows the total unweighted frequency content of the exhaust system. Under normal trail riding conditions, engine speeds are typically between 3500 and 8000 RPM. These speeds cause the exhaust ports to open and close at a frequency of 117 to 267 Hertz, respectively. The increased frequency content recorded from the pipe location as seen in Figure 7 reflects this. However, the frequency

content recorded from the muffler location does not. Figure 7 shows the total frequency content after the expansion pipe is at higher frequencies than before the expansion pipe.

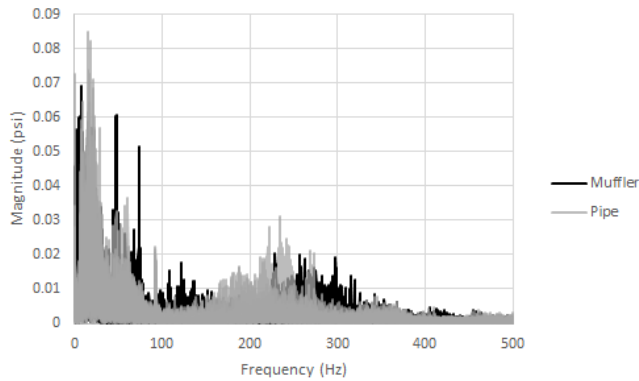


Figure 7: Total frequency content before and after the expansion pipe at all engine operating speeds.

Equation 2 shows gives the dBA scale weighting where $R_A(f)$ is defined in Equation 3.

$$A(f) = 20 \log_{10}(R_A(f)) + 2.00 \quad (\text{EQ 2})$$

$$R_A(f) = \frac{12194^2 \cdot f^4}{(f^2 + 20.6^2) \sqrt{(f^2 + 107.7^2)(f^2 + 737.9^2)} (f^2 + 12194^2)} \quad (\text{EQ 3})$$

As can be seen in Figure 8, the muffler should attenuate frequencies between 220 and 320 Hertz, as these are the highest magnitude sounds within the range of frequencies recorded. Selection of sound reduction techniques for higher frequencies were carried out using the impedance tube and microphones. The data acquisition unit used in pressure data collection was unable to sample at higher rates, so higher frequencies could not be tested with this method.

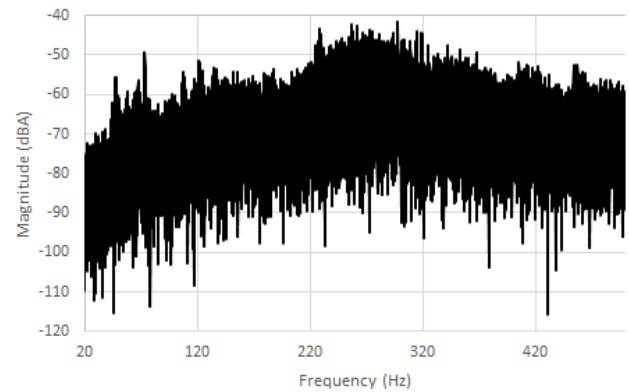


Figure 8: Total frequency content after the expansion pipe at all engine operating speeds weighted with the dBA scale.

Muffler Design

A major part of noise reduction takes place in the snowmobile's muffler system. The muffler used this year is a new design and concept compared to the teams 2017 machine. The implementation of a catalyst into the system was a major space constraint, adding additional challenges to the muffler's overall design. The catalyst generally requires exhaust gas temperatures upwards of 572 °F as a minimum operating temperature, but preferably the catalyst would be around 900 °F to efficiently convert emissions, meaning that it would have to be placed upstream of most of the other exhaust components [2]. The location chosen was at the entrance to the muffler after the exit of the tuned pipe. Due to the design of the AXYS chassis and packaging concerns, a bottom-side exit system similar to the stock muffler was chosen. For weight and cost reasons, an electric start system was not installed on the snowmobile, allowing for the exhaust design team to utilize the space that would have otherwise been used by a battery. This would be a major benefit, as a muffler's ability to reduce exhaust noise is highly dependent on its volume [3]. Given in Figure 9 is a SolidWorks section rendering of the muffler design.

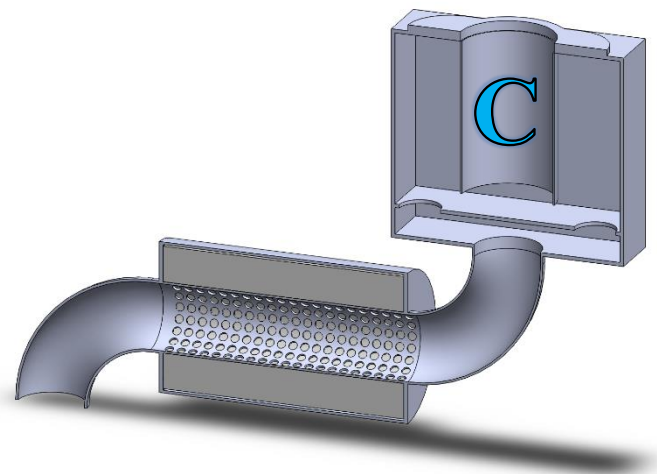


Figure 9: Full SolidWorks rendering of exhaust muffler system. Catalyst location is marked with a letter C.

A three-chamber design was chosen as the basis for the muffler. The first chamber was designed to slow down and mix the flow coming out of the catalyst. This chamber also acts as a barrier between the catalyst and other components on the sled that may be affected by high levels of radiated heat. After slowing and mixing, the flow enters the second chamber. The second chamber is designed to make use of destructive interference to reduce exhaust noise by directing two flows towards each other. The third chamber of the muffler contains a perforated tube expansion with exhaust packing material, designed to convert the sound energy of the flow into thermal energy in the packing, and then exit the snowmobile towards the ground. This bottom exit design will direct exhaust gases down towards the snow, further dissipating sound energy.

Using ANSYS Fluent and CFX software, full flow simulations were conducted to visualize the gas flows and pressure generation. Figure 10 shows the pressure distribution as exhaust gases flow from inlet to outlet. The simulation showed that the muffler produced 0.692 psi of peak backpressure, which the design team deemed to be acceptable.

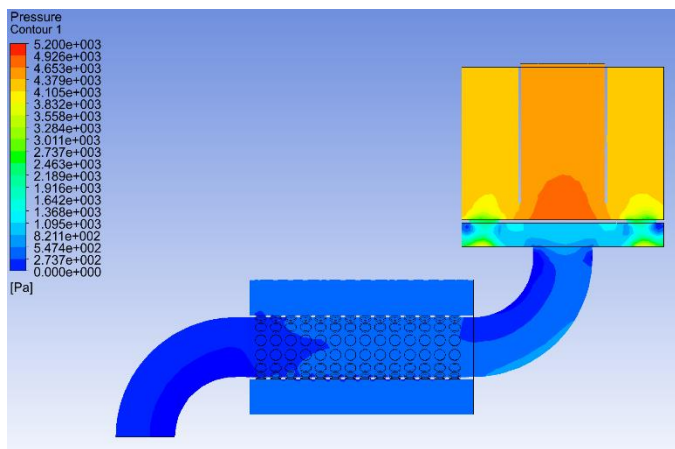


Figure 10: Pressure distribution of muffler shown by ANSYS Fluent simulation.

Simulated streamlines for the muffler design are shown in Figure 11. The simulation shows the destructive interference in the second section of the muffler, as well as the mixing and slowing of the entering exhaust gases.

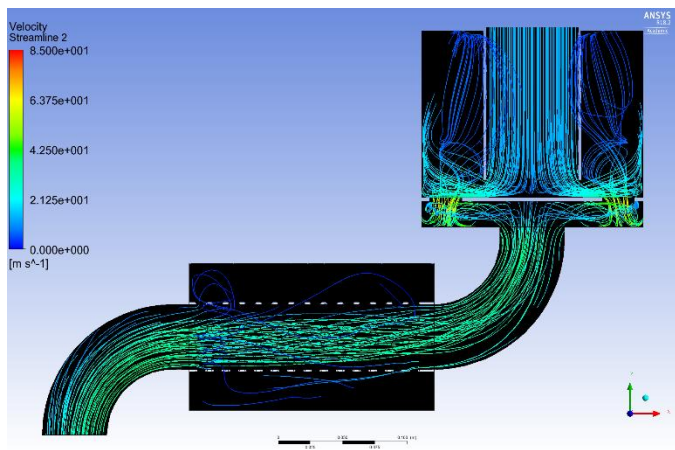


Figure 11: Flow simulation performed in ANSYS.

Impedance Tube

Several improvements were made to the impedance tube used for the 2017 Clean Snowmobile competition [4]. These include using a two-microphone setup, adding operational amplifiers (op-amps) to increase the signal from the microphones, and providing a sinusoidal excitation across the speaker instead of the square wave that had been used previously. The improvement in both test speed and fidelity allowed the team to diagnose problems and test more samples at a faster rate than the previous design allowed.

In last year's design, the microphone was placed at the end of the quite side of the tube. The two-microphone design has one microphone before the sample and the second microphone after the sample, see Figure 12. The microphones are mounted flush with the wall of the impedance tube in order to reduce their effect on the plane wave in the tube [5]. This also allows for different anechoic termination at the end of the tube to reduce the amount of sound reflected by the end of the impedance tube. Several pieces of foam were used as the anechoic termination in the following material tests.

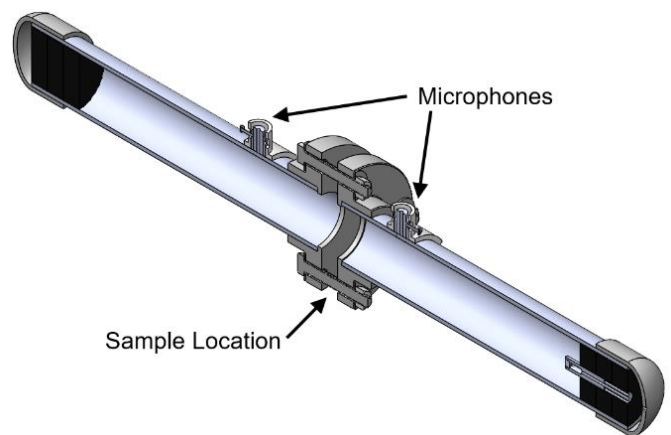


Figure 12: Impedance Tube design including two microphones.

The microphone was directly connected to the analog input on the NI myRio last year. The sensitivity of the microphone used last year was -42 dB which corresponds to a change of 0.008 V/Pa. The analog input on the myRio has a resolution of 0.002 V. Low voltages like the output from the microphone are susceptible to electrical noise. An op-amp increases the voltage from the microphone by a factor called the gain. The op-amps for the microphones were design to have a gain of 100. The analog input reads the amplified signal which effectively increases the sensitivity of the microphone. The gain is then removed from the signal numerically after the analog input reads the signal.

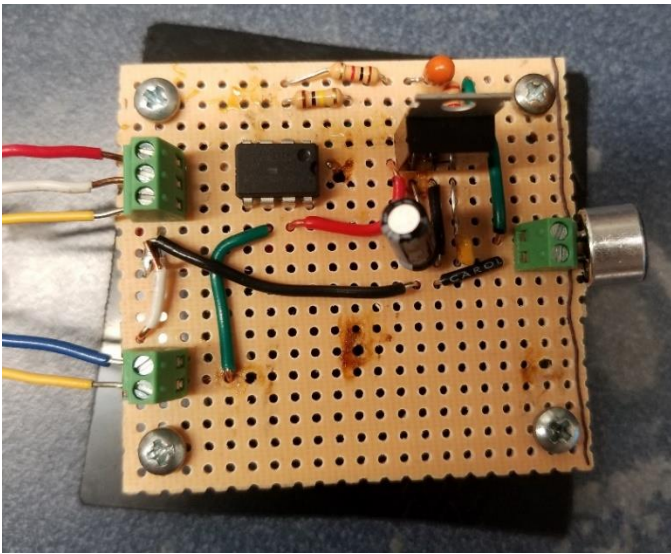


Figure 13: One of the op-amps used with the microphones.

For the 2017 competition design cycle, the speaker in the impedance tube was driven by a square wave from the pulse width modulation feature on the digital output of the myRio. When the square wave was used to drive the speaker, the output from the speaker had higher order frequencies superimposed upon it as seen in Appendix A-1. A sine wave is theoretically composed of many sine waves superimposed upon each other. The lowest frequency sine wave in the composition being the intended frequency. When a sinusoidal wave was applied across the speaker, see Appendix A-2, the speaker output was closer to the desired shape. A sine wave was implemented in in LabVIEW. The analog output was updated at a rate of 10 kHz.

Material Testing

Several coatings were investigated this year. The coatings were applied to 1/8 inches thick ABS sheets. The absorption coefficient test was run 5 times for each material. The absorption coefficient was then found by averaging the five runs. As seen in Figure 14, the coating demonstrated very similar behavior except at 1 kHz. The absorption coefficient of close to one everywhere except 1 kHz indicates that the ABS sheet absorbed too much of the incident acoustical energy for there to be significant acoustical energy on the other side. The effects of the coatings were not significant enough to improve the absorption coefficient. At 1 kHz, all the samples tested deviate from the absorption coefficient of one. Since all the samples deviate at the same point, it is likely to be a resonance specific to the tube. If the resonance increases the pressure in the tube, this would make the tube louder. A greater acoustical pressure drop across the sample would increase the effect of the coating. The Flex Seal and caulk continue to absorb acoustical energy the best at the 1 kHz frequency. Since the caulk is difficult to apply in an even layer, the Flex Seal was selected.

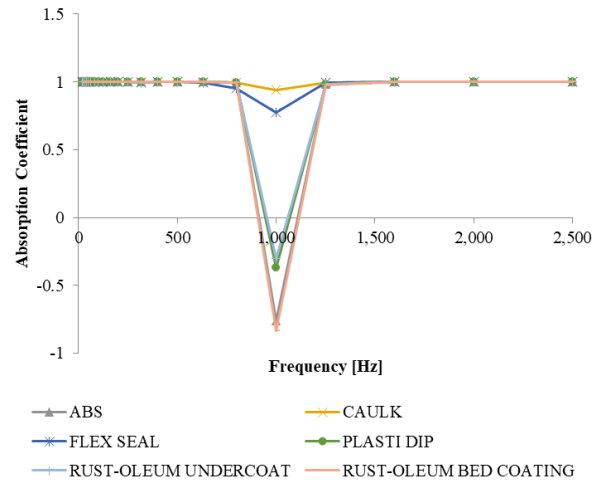


Figure 14: Absorption coefficients for the six materials tested.

Investigation of Helmholtz Resonators

Helmholtz resonators were being considered for use in the custom exhaust for the snowmobile. For various reasons, the design with the resonators was deemed unfeasible for this year's competition. A few resonators were fabricated, and their acoustic performance was investigated. Helmholtz resonators are a notch reject type of filter. It is also possible for the Helmholtz resonator to amplify frequencies surrounding the rejected frequency.

Methods and Materials

The impedance tube was used to perform the testing on the resonators. A speaker was placed in one end of the tube. The Helmholtz resonator was installed between the pipe flanges of the impedance tube with the use of adapter plates, see Figure 15. Two microphones were used to record sound (Model# CMC-6027-24T). One was located before the 2-inch metal pipe section on the speaker side, and the other was located on the quiet side after the metal pipe. The orange plastic pieces in Figure 15 are the mounts for the two microphones. On the quiet side of the impedance tube, the end cap was removed to reduce resonance and reflection in the tube.



Figure 15: Picture showing a Helmholtz resonator being tested in the impedance tube.

LabVIEW and the NI myRio were utilized for creating the signal to the speaker, recording voltages from the microphones, and data processing. The NI myRio analog output generated a sine wave for the speaker. The analog output was updated at a rate of 10 kHz. The 10 kHz rate is the practical update limit that the myRio can attain for analog outputs. The target frequency ranged from 100 Hz to 2500 Hz inclusive in increments of 25 Hz. The target frequency was played for 1 second. A Lepai LP-2020A+ audio amplifier was connected to the audio output on the myRio to drive the speaker. The volume setting on the amplifier was kept constant for all resonator tests. Due to the low output voltages of the microphones, op-amps were used to amplify the microphone signals. Both op-amps had a theoretical gain of 100 with a rail voltage of ± 12 volts. The microphones were sampled at 20 kHz. The multiplexer on the myRio was able to maintain sampling both microphones at a rate of 20 kHz, but was unable to go significantly faster without experiencing an uneven number of clock ticks per cycle or being late for the next cycle. Considering the highest frequency of interest during the frequency sweep in 2.5 kHz, the sample rate (20 kHz) is 8 times faster. This satisfies the Nyquist sampling criterion.

After the sweep method described above was completed, the percussive method was employed. With the Helmholtz resonator in the impedance tube, a soft handled screw driver was used to excite the end of the volume on the resonator. The induced frequencies in the tube were measured by the microphone on the quiet side of the tube. A sampling rate of 20 kHz was used. The microphones and op-amps were the same as the ones used in the sweep method.

When both the sweep and percussive tests were performed on the resonator, the resonator was replaced with the next resonator. Three resonators were tested in this manner. The small resonator had a theoretical reject frequency of 170 Hz with room temperature air. The medium resonator had a theoretical reject frequency of 100 Hz at room temperature. The large resonator was designed to reject 33 Hz at room temperature.

Analysis

The sound pressure level (SPL) before and after each resonator are shown in 16 and 17. The post-resonator microphone exhibits a large decrease in SPL at 425 Hz for all three resonators. Since this behavior is seen across all the resonators that were tested, it is highly

Page 7 of 9

2/18/2018

likely that this decrease in SPL is related to a resonance in the quiet side of the tube. Therefore, this data point can be ignored.

The absorption coefficient was calculated for each frequency played in the sweep. The absorption coefficient is defined as the change in acoustical energy across the resonator over the total incident acoustical energy, see Equation 4.

$$\alpha = \frac{\Delta E}{E_{Incident}} = \frac{E_{Incident} - E_{After}}{E_{Incident}} \quad (EQ 4)$$

, where α is the absorption coefficient, $E_{Incident}$ is the acoustical energy before the resonator, and E_{After} is the acoustical energy after the resonator [4]. As shown in 16, the absorption coefficient for the medium resonator has minimum at 1 kHz. When the absorption coefficient is less than zero, the frequency is amplified. For the medium resonator at 1 kHz, the resonator acts as an amplifier and increases the volume.

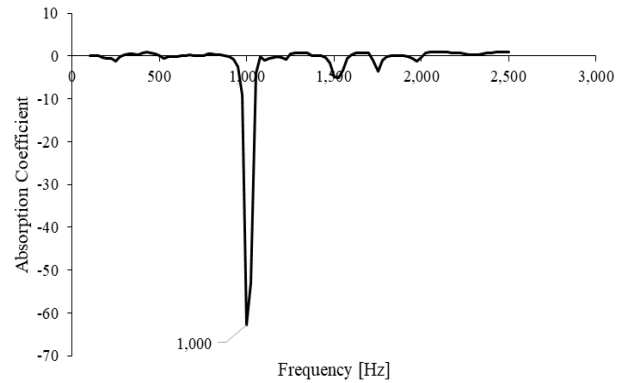


Figure 16: Absorption coefficient for the medium resonator. The resonator increases the SPL at 1,000 Hz.

The transmission loss across the resonators were also calculated. The transmission coefficient, τ , of a material is defined as the ratio of power through a material, P_{Out} , to the power incident to the material, P_{In} [5].

$$\tau = \frac{P_{Out}}{P_{In}} \quad (EQ 5)$$

The amount of power transmitted by a pressure wave is a function of the area perpendicular to the travel of the wave (A), the amplitude of the pressure wave at a given frequency (p), the density of air (ρ), and the speed of sound (c).

$$P = \frac{A p_{Amp}^2}{\rho c} \quad (EQ 6)$$

Combining equation 5 and 6.

$$\tau = \frac{\frac{A p_{Out}^2}{\rho c}}{\frac{A p_{In}^2}{\rho c}} = \frac{p_{Out}^2}{p_{In}^2} = \left(\frac{p_{Out}}{p_{In}} \right)^2 \quad (EQ 7)$$

The density of air and speed of sound were assumed to not vary significantly during a test as the atmospheric pressure and ambient temperature change at a slow rate compared to the 1 second sample time at each frequency. From the transmission coefficient, the transmission loss can be calculated [5].

$$TL = 10 \log_{10} \left(\frac{1}{\tau} \right) \text{ in dB} \quad (EQ 8)$$

Figure 17 shows the transmission loss across the medium resonator. A positive transmission loss represents a frequency at which the resonator attenuated noise. The negative values show where the resonator amplified noise.

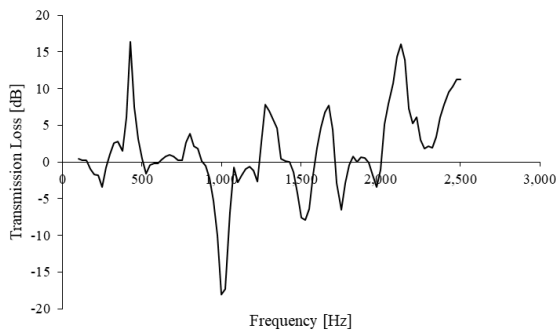


Figure 17: Transmission loss across the medium resonator.

Using the absorption coefficient versus the transmission loss to evaluate the performance of a resonator yields different results. The graph of absorption coefficient, see Figure 16, leads one to believe that the resonator is ineffective at attenuating noise. Instead, the resonator mainly amplifies the noise at 1 kHz. However, this analysis is misguided since the absorption coefficient should never go over one. At an absorption coefficient of one, all of the incident energy is dissipated with no energy making it past the resonator. However, if the resonator is amplifying the noise, the absorption coefficient will tend towards negative infinity as the amplification increases. Hence, the absorption coefficient is a good indicator of what frequencies a resonator amplifies at and a poor indicator of what frequencies it attenuates at. It should be noted that the absorption coefficient works better with solid material sample in the tube since amplification should not theoretically occur. The transmission loss presents a better view of resonator attenuation than the absorption coefficient does. Instead of capping attenuation at a maximum value of one, the transmission loss allows the scaling of attenuation and amplification over a wider range that highlights both cases well. In Figure 17, the 1 kHz amplification can still be seen, but the attenuation is also readily apparent. The small and large resonator data was comparable to the data shown in Figure 16 and Figure 17.

From an exhaust design perspective, the amplification of certain frequencies poses a problem when the engine speed changes during operation. For an engine that will be used at a constant engine speed, the amplification caused by the Helmholtz resonators can be designed to occur at frequency that the engine does not produce much noise at. Hence, the resonator can attenuate at a specific frequency and not have a significant amount of noise amplified at the other frequencies. However, when the engine speed varies during operation, the frequencies produced by the engine will also vary. This means that at certain engine speeds the Helmholtz resonator will amplify specific frequencies that are of significant volume before amplification. Due

to this concern, using Helmholtz resonator with a variable speed engine can be counterproductive.

Summary/Conclusions

In conclusion, the team utilized new project management strategies to ensure the on-time delivery of projects, improved emissions with the inclusion of a new, larger catalyst, designed a new custom muffler and selected sound absorbing coatings to reduce noise.

References

1. 2018 SAE Clean Snowmobile Challenge Rule Book
2. Lee, S., Bae, C., Lee, Y., and Han, T., "Effects of Engine Operating Conditions on Catalytic Converter Temperature in an SI Engine," SAE Technical Paper 2002-01-1677, 2002, <https://doi.org/10.4271/2002-01-1677>.
3. Shital Shah, Saisankaranarayana Kuppili, Kalyankumar Hatti, and Dhananjay Thombare "A Practical Approach towards Muffler Design, Development, and Prototype Validation," SAE International, doi: 2010-32-0021 20109021
4. "Reducing Exhaust Emissions and Investigating Sound Deadening Materials for a Two Stroke Snowmobile". *University of Minnesota: Clean Snowmobile Team*. February 2017. Accessed February 17, 2018.
5. Satyajeet P Deshpande and Mohan D Rao, "Development of a Low Cost Impedance Tube to Measure Acoustic Absorption and Transmission Loss of Materials," *American Society for Engineering Education* (2014, June)

Acknowledgments

The University of Minnesota-Twin Cities Clean Snowmobile Team would like to thank our sponsors, whose support was instrumental in our success this year: Polaris, Heraeus, Camso, Hayes, Woody's, Dynojet Research, ANSYS, SOLIDWORKS

We would also like to thank the University of Minnesota College of Science and Engineering, Department of Mechanical Engineering, and our faculty advisor, Dr. William Northrop.

Definitions/Abbreviations

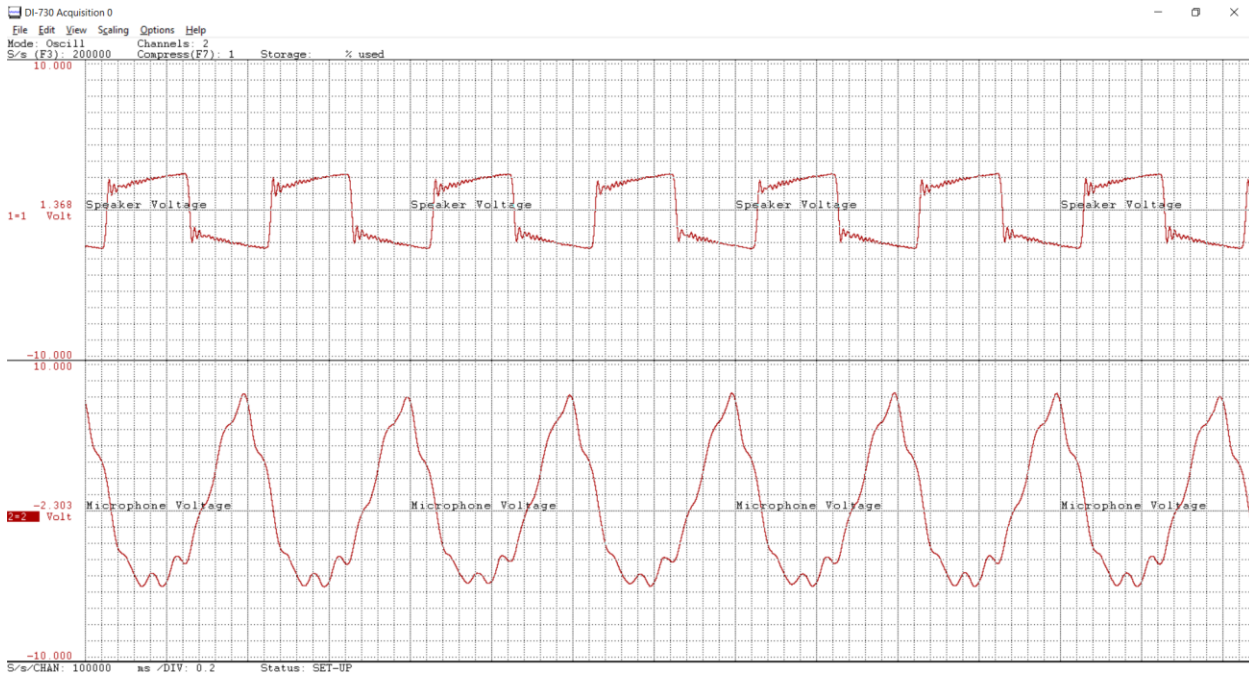
RPM – Revolutions per minute

HC - Hydrocarbons

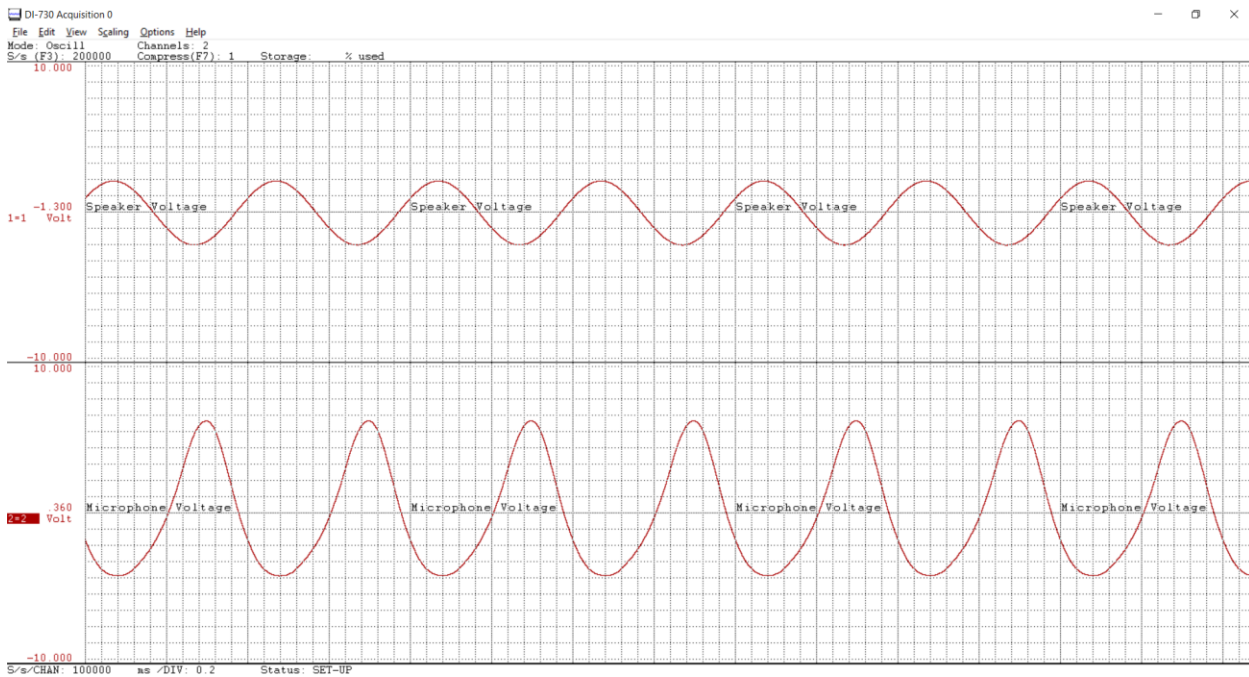
NO_x – Nitrides of Oxygen

CO – Carbon monoxide

Appendix A



Appendix A-1: Speaker output when square wave excitation is applied



Appendix A-2: Speaker output when sinusoidal excitation is applied